Segmental Diffusion in Attractive Polymer Nanocomposites: A Quasi-Elastic Neutron Scattering Study

Eric J. Bailey[†], Philip J. Griffin[†], Madhusudan Tyagi[§,‖], and Karen I. Winey*[,†]

[†] Department of Materials Science and Engineering, University of Pennsylvania, Philadelphia, Pennsylvania 19104, United States

[§] Center for Neutron Research, National Institute of Standards and Technology, Gaithersburg, Maryland, 20899, United States

[‖] Department of Materials Science and Engineering, University of Maryland, College Park, Maryland, 20742, United States

*Author to whom correspondence should be addressed. Electronic address: winey@seas.upenn.edu

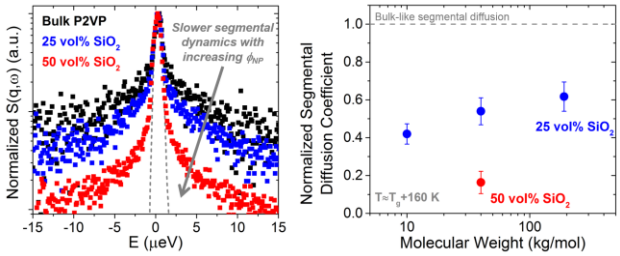

For Table of Content use only

Abstract:

We present a systematic study of segmental dynamics in model attractive polymer nanocomposites comprising poly(2-vinyl pyridine) (P2VP) and 26-nm diameter colloidal silica nanoparticles (NPs) using quasi-elastic neutron scattering (QENS). Unlike most dynamic measurements, QENS provides both spatial and temporal information on small length scales (~1 nm), fast time scales (~1 ns), and therefore at temperatures far above the glass transition. We find that on these length and time scales, P2VP segmental motion is well-described by classic translational diffusion even under extreme confinement, where the average interparticle spacing is on the order of the Kuhn length. The average segmental diffusion coefficient decreases monotonically with increasing NP concentration by up to a factor of ~5 at the highest NP concentrations (50 vol%). Interestingly, this reduction in segmental dynamics is very weakly dependent on P2VP molecular weight spanning the unentangled (10 kg/mol) to the highly entangled regimes (190 kg/mol). This stands in contrast to the well-documented molecular weight effect on segmental dynamics in attractive polymer nanocomposites at lower temperatures.

Introduction:

The addition of nanoparticles (NPs) to a polymer matrix, forming a polymer nanocomposite (PNC), can significantly enhance the thermal, mechanical, and functional properties of the host matrix.[1,2] Furthermore, PNC materials have wide-ranging tunable properties that can be dominated by the polymer, the nanostructured filler, or the interfacial region. As such, they are appealing materials for a variety of fields. Several questions still exist regarding the dynamic properties of free and interfacial chains. Polymer dynamics in polymer nanocomposites and polymer melts significantly influence or dictate their processability, applications, glass transition temperature (T_g), and various macroscopic properties (such as creep, toughness, and transport). In addition, due to the large surface area to volume ratio of NPs, PNCs are a model system to study the perturbation to polymer dynamics caused by a solid interface.

At the largest length scale, elastic recoil detection measurements have been conducted to probe center-of-mass polymer chain diffusion in PNCs with NPs that are athermal[3], attractive[4], grafted[5] and anisotropic[6–9]. This work has recently been reviewed.[10] Similar dynamics were probed using nuclear-magnetic-resonance techniques as well.[11] On a smaller length scale, segmental dynamics in PNCs have received more attention due to their relevance toward ion transport, small molecule separation, and the glass transition. This topic has also recently been reviewed from different perspectives.[12–16] However, additional fundamental studies are needed to explore the complex parameter space and understand the underlying physics of interfacial and confined polymer dynamics.

There are several methods that can be used to analyze segmental dynamics including nuclear magnetic resonance (NMR), dynamic mechanical measurements (DMA), broadband dielectric spectroscopy (BDS), temperature-modulated differential scanning calorimetry (TMDSC), neutron spin echo (NSE) and quasi-elastic neutron scattering (QENS). The approximate timescales associated with many of these measurement techniques, as they pertain to segmental dynamics, are schematically represented in Figure 1. Also included in Figure 1 is a characteristic polymer segmental relaxation (α-process) curve following Vogel-Fulcher-Tammann (VFT) temperature dependence,

$$\tau(T) = \tau_0 \exp\left(\frac{B}{T - T_0}\right) \quad (1)$$

where τ_0, B and T_0 are fitting parameters related to high temperature relaxation time, fragility, and Vogel temperature, respectively. To probe the α-process with a particular technique, the measurement temperature must be chosen such that the α-process falls within the accessible temporal window of the technique. For example, TMDSC measurements are particularly useful for measurements near T_g (~0.5 – 50 s) and BDS is useful for its coverage of over 6 decades in relaxation times at temperatures above T_g.[17] QENS, the focus of this paper, has the advantage of spanning even shorter time scales while providing simultaneous temporal and spatial information to capture the timescales and geometries of measured motions.

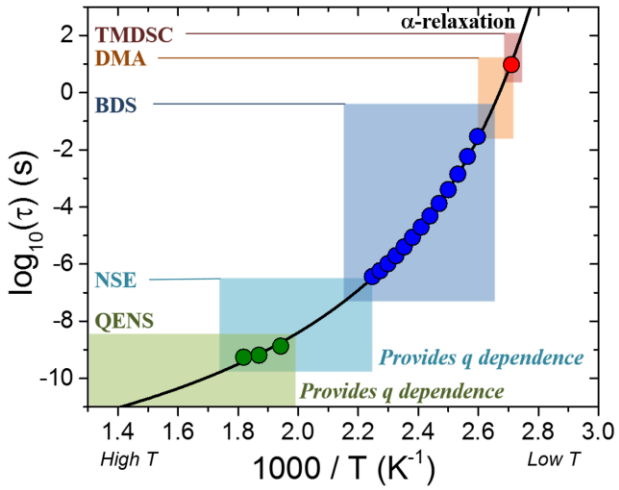

Figure 1: Primary segmental relaxation times (α-process) of bulk polymer as a function of inverse temperature. Approximate time scales for five techniques, and their corresponding temperatures, are depicted by shaded regions along the relaxation curve. Not depicted is NMR, which is used to characterize various polymer dynamic processes over several orders of magnitude. Black line represents VFT fit for bulk 40 kg/mol P2VP measured via TMDSC (red circle), BDS (blue circle), and QENS (green circle).

QENS measurements have been performed on filled rubber[18,19], polymer/layered silicate nanocomposites[20,21], and other PNC systems[22–28]. For example, in a PNC where free chains were removed by extraction, Roh et al. found slower relaxations and increased dynamic heterogeneity for 1,4-polybutadiene segments near aggregated carbon black NPs compared to segments in bulk polymer.[19] For crystalline poly(dimethyl siloxane)/SiO_2 PNCs, multiple polymer processes were analyzed and generally, bulk-like dynamics were measured below the polymer glass transition while slow dynamics attributed to

interfacial polymer were identified at higher temperatures.[23] Additionally, QENS and NSE experiments on low molecular weight polyethylene glycol and SiO_2 (an attractive interaction) shows physically adsorbed chains are dynamically active with pico-second segmental dynamics at 413 K, but slowed relative to bulk.[26]

Recently, polymer nanocomposites comprising poly(2-vinyl pyridine) (P2VP) and colloidal silica (SiO_2) have emerged as model systems for studying the properties of attractive PNCs.[29–31] In these systems, it has been experimentally shown that a physically adsorbed bound polymer layer of thickness ~R_g spontaneously forms on the NP surface in solution and persists in the melt state.[30] On the atomic level, hydrogen bonding between the nitrogen in P2VP and native hydroxyl groups on the surface of SiO_2 was directly observed by sum frequency generation and X-ray photoelectron spectroscopic techniques.[31] The segmental dynamics of P2VP/SiO_2 PNCs have also been studied by dielectric spectroscopy as a function of NP concentration[29], NP size[32], polymer molecular weight[33], and interfacial bonding strength[34]. An interfacial layer on the order of a few nanometers with suppressed segmental dynamics has been identified in these experiments, and the degree to which the dynamics are suppressed increases with decreasing polymer molecular weight, among other characteristics.[15,31,33] Analysis of small-angle X-ray scattering[33], pycnometry data[31], and various spectroscopic techniques[31] suggest that shorter chains pack more efficiently at the NP surface, leading to a greater fraction of physisorbed segments, slower interfacial dynamics, and a thicker interfacial layer. Despite this progress, a recent review by Sokolov et al. highlighted that the impact of temperature on the structure and dynamics of interfacial polymer, and whether the molecular weight effect is a kinetically trapped phenomena or an equilibrium state, remains an open question.

In this article, we present a systematic study of segmental dynamics in attractive polymer nanocomposites comprising P2VP and colloidal SiO_2 NPs using TMDSC ($T \sim T_g$) and QENS ($T \sim T_g$+150K). We show that motions of P2VP segments on ~1 nm length scales and ~1 ns time scales are well described by classic translational diffusion, even at NP concentrations of ~50 vol% where the average interparticle spacing is ~2 nm. The average segmental diffusion coefficient decreases with increasing NP concentration by up to a factor of ~5 and is mostly independent of temperature over the studied temperature range. In contrast to the well-documented molecular weight dependence of segmental diffusion in the deeply

supercooled regime, our measurements of the same dynamic process at higher temperatures show reduced segmental dynamics that are largely independent of matrix molecular weight. Finally, by comparing TMDSC, BDS, and QENS, our results suggest that temperature has a significant impact on the NP-induced perturbation to segmental dynamics in PNCs and highlights the unique and complementary insights that can be provided by QENS.

Experimental Section:

Materials: All poly(2-vinylpyridine) (P2VP) was purchased from Scientific Polymer Products, Inc. and used as received. To study the molecular weight dependence of interfacial dynamics, unentangled (10 kg/mol), lightly-entangled (40 kg/mol), and well-entangled (190 kg/mol, $M/M_e \approx 11$) P2VP were also studied.[30] Throughout this paper, these samples will be referred to as 10, 40, and 190 kg/mol although the weight average molecular weights were measured using GPC and are listed in Table 1. All measured molecular weight dispersities were < 1.3. To study the role of NP concentration and temperature on polymer segmental dynamics, PNCs were fabricated with 40 kg/mol P2VP. Silica NPs were synthesized following the modified Stöber[35,36] method with a log-normal geometric mean diameter (d_{NP}) of 26.1 nm and standard deviation standard deviation $e^{\sigma} = 1.2$ as determined by analysis of transmission electron micrographs (TEM).[30]

Table 1: Nanocomopsite details including P2VP molecular weight, NP concentration (ϕ_{NP}), calorimetric T_g of bulk polymer and PNCs, measurement temperatures for QENS, and degradation temperature taken as the temperature of 5% mass loss in bulk polymer. All P2VP molecular weight dispersities are < 1.3.

Molecular Weight (kg/mol)	ϕ_{NP} (vol%)	Bulk T_g (K)	PNC T_g (K)	ΔT_g (K) $T_g^{PNC} - T_g^{bulk}$	QENS Temperature (K)	Bulk Degradation Temperature (K)
9.9	24.2	362.4	366.6	4.2	525	615
39.3	25.3	369.0	370.2	1.2	550, 535, 515, 480	626
188	25.4	376.2	376.7	0.5	535	626
39.3	52.7	369.0	372.3	3.3	550, 535, 515	626

PNC Preparation: PNC samples were made by solution mixing of P2VP/MeOH ($c_{polymer}$ < 2 wt %) with the appropriate amount of SiO_2/EtOH ($c_{NP} \approx 15$ mg/mL) to achieve desired NP concentrations (25 or 50 vol%). Solutions were continuously stirred for at least 12 hours to ensure homogeneous dispersion of NPs. The P2VP/SiO_2 mixture in solution has good dispersion as found by dynamic light scattering, where a single peak at ~d_{NP} was observed. Bulk polymer and PNC solutions were drop casted in Teflon dishes

and dried in ambient conditions for 24 hours, then annealed at T_g+60 K for at least 12 hours under vacuum. Representative TEM micrographs illustrate that NPs remain well-dispersed in the as-dried PNCs (Figure S1). The presence of a physically adsorbed bound layer in P2VP/SiO_2 PNCs is known to promote good NP dispersion and prevent NP-NP aggregation.[30,34,37]

Thermogravimetric Analysis (TGA): Polymer degradation behavior and NP concentrations were measured via TGA using a TA instruments SDT Q600. For each measurement, a sample of 5-10 mg was placed in a platinum pan and heated from 300 K to ~1100 K at a rate of 5 K/min under air purge. NP concentrations listed in Table 1 were calculated with the TGA results and densities of 1.2 and 2.3 g/cm^3 for P2VP and SiO_2, respectively.[33]

Temperature-Modulated Differential Scanning Calorimetry (TMDSC): The calorimetric glass transition was measured via TMDSC with a TA Instruments Q2000. All measurements were made upon cooling a sample of ≥ 5 mg of polymer at a rate of 5 K/min with a modulation time of 30 sec and amplitude of ±0.5 K over a temperature range of T_g ± 60 K. T_g was defined as the inflection point of the heat flow thermograms and all results were reproduced.

Broadband Dielectric Spectroscopy (BDS): Segmental dynamics of bulk P2VP was measured with BDS using a Solartron ModuLab XM MTS with the femto-ammeter accessory. Polymer films were placed between steel electrodes and separated with 50 μm silica spacers. Samples were annealed in the cryostat at 420 K until the imaginary permittivity spectra stopped changing. Isothermal frequency sweeps from 10^{-1} – 10^6 Hz were measured every 5 K between 380 and 450 K on cooling. Measurements were made after heating again to ensure reproducibility.

Quasi-Elastic Neutron Scattering (QENS): Inelastic neutron scattering measures the double differential scattering cross-section ($d^2\sigma/d\Omega d\omega$), which is related to the probability that a given incident neutron is scattered into a solid angle $d\Omega$ with an energy transfer $d\omega$. The double differential scattering cross-section has incoherent and coherent contributions, each of which can be expanded and related to the dynamic structure factors:

$$\frac{d^2\sigma}{d\Omega d\omega} = \left(\frac{d^2\sigma}{d\Omega d\omega}\right)_{inc} + \left(\frac{d^2\sigma}{d\Omega d\omega}\right)_{coh} = \frac{k_1}{k_0 4\pi} N \left[\sigma_{inc} S_{inc}(q,\omega) + \sigma_{coh} S_{coh}(q,\omega) \right] \quad (2)$$

where k_0 and k_1 are the magnitude of incident and final wave vectors, respectively, N is the number of nuclei, σ is the incoherent and coherent scattering cross sections of the nuclei, and S(q, ω) is the incoherent and coherent dynamic structure factors. Because σ_{inc}^{H} (~80 barns) is much larger than all other atoms in this system (σ_{other} < ~6 barns), we can generally assume that the signal is dominated by the incoherent contribution to Equation 2.[38] For example, using Equation 2, ~90% of the signal in P2VP is incoherent and even at our maximum SiO_2 concentration of 50 vol%, the polymer accounts for ~63% of the total scattering.[38] $S_{inc}(q, \omega)$ is the time and space Fourier transform of the self-part of the van Hove correlation function and combines spatial ($q=k_1-k_0$) and temporal (ω) information for correlations between the single nuclei.[39] Quasi-elastic neutron scattering measures $S_{inc}(q, \omega)$ centered at ω=0, and is typically used to probe diffusive motions on molecular length scales.

QENS measurements were made at the High-Flux Backscattering Spectrometer (HFBS, NG2) at the NIST center of neutron research in Gaithersburg, MD, USA.[40] Samples containing at least 200 mg of polymer were folded and sandwiched into aluminum foil and placed in cylindrical aluminum cans for measurements. Each sample was approximately 50 μm thick.

First, in a fixed window scan (FWS), the elastic scattering intensity $S_{inc}(q, \omega=0)$ was measured as a function of temperature, starting at 50 K with a heating rate of 1 K/min. Second, $S_{inc}(q,\omega)$ was measured at select temperatures over a q-range of 0.25–1.75 $Å^{-1}$ and an energy range spanning -17–17 μeV (with a resolution of 0.8 μeV as defined by the elastic scattering of vanadium at 50 K). These q- and energy ranges correspond to molecular dynamic processes with length and time scales of approximately 3–25 Å and 40 ps–2 ns, respectively. The measurement temperatures were guided by extrapolating dielectric relaxation times (similar to Figure 1) and further refined by choosing a temperature where mean squared displacements measured via FWS were ~7 $Å^2$ or at least 3 $Å^2$ for the lowest temperature measurements. QENS spectra

were collected for 12 hours under vacuum after a 30-minute equilibration at the measurement temperature. Analysis was primarily conducted in DAVE software.[41]

In this PNC system, relatively high temperatures are necessary to observe the segmental diffusion process in the dynamic window of QENS and are mostly unexplored. The thermal degradation temperatures of bulk P2VP, as defined by the temperature at which 5 wt% polymer is lost in TGA are >600 K (Table 1). (Full thermograms are presented in Figure S2.) The maximum temperature of FWSs and QENS measurements are sufficiently below the onset of thermal degradation, by at least 75 K (Table 1). Nevertheless, a thorough analysis of molecular weight (GPC), T_g (TMDSC) and thermal degradation (TGA) of samples after QENS measurements are presented in Section 9 of Supporting Information. Although the thermal degradation behavior did not change after measurements (Figure S10), the molecular weight and glass transition temperature decreased slightly (Table S1 and Figure S9, respectively). It is important to note that molecular weights measured after QENS measurements are still categorically different and span the unentangled to well-entangled regimes. These changes in chain length and T_g are expected from slight polymer degradation, but do not affect the reported measurements of segmental dynamics or main conclusions of this work.[42] To confirm this, Section 9 of Supporting Information also includes a time-dependent analysis of QENS, showing the sample measurement was the same at the beginning and end of the experiment. This result demonstrates the reliability of these QENS measurements.

Results:

The glass transition temperature (T_g) of P2VP/SiO_2 PNCs as measured by TMDSC are shown in Figure 2 and listed in Table 1. The absolute T_g shown in Figure 2 increases with P2VP molecular weight (MW) and NP concentration (Figure 2, 40 kg/mol). It is well-established that the addition of highly attractive NPs causes an increase in T_g resulting from the slowing down of the primary structural relaxation (α-process) at the NP-polymer interface.[15] As such, it is expected that increased NP concentration causes an increase in T_g due to the larger volume fraction of 'interfacial' polymer affected by the NP surface. Furthermore, the impact of the same concentration of NPs is much more pronounced for unentangled polymer (~4 K for 10 kg/mol P2VP) than in well-entangled polymer (<1 K for 190 kg/mol P2VP). This increased perturbation for lower molecular weight PNCs has recently been reported and described by differences in interfacial packing.[31,33,34] Importantly, our measurements agree with calorimetric measurements of T_g on similar systems.[29,33,34]

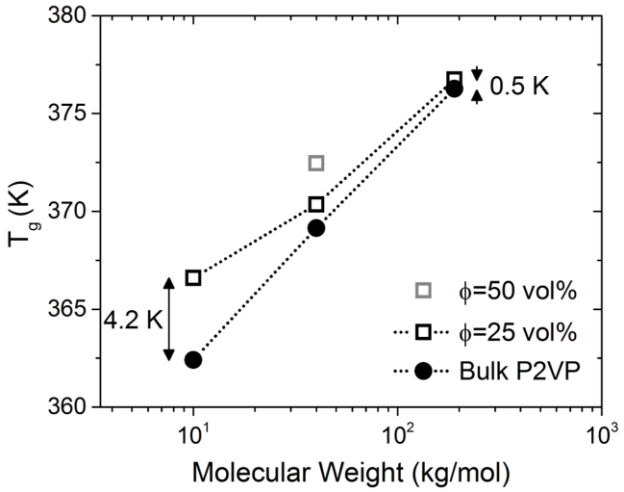

Figure 2: Absolute glass transition temperature (T_g) as measured by TMDSC for each molecular weight and NP concentration studied. Difference in T_g between P2VP with 25 vol% SiO_2 and bulk P2VP is labelled for 10 and 190 kg/mol P2VP.

Effect of NP concentration on segmental mobility: To further understand segmental dynamics in these PNCs at elevated temperatures, we use neutron scattering to measure PNCs with modest molecular weight (lightly entangled, 40 kg/mol) and NP concentrations of 25 and 50 vol%. First, the elastic scattering

of each sample was measured as a function of temperature from 50 K to 550 K in a FWS. The mean-squared displacement ($\langle x^2 \rangle$) was determined using the Debye-Waller approximation, as discussed in Section 3 of Supplemental Information.[43,44] Figure 3 displays the fitting results where $\langle x^2(T) \rangle$ is shown relative to $\langle x^2(T=T_g^{bulk} - 100\ K) \rangle$ and the temperature is plotted relative to T_g^{bulk}. Data without normalization is provided in Figure S3.

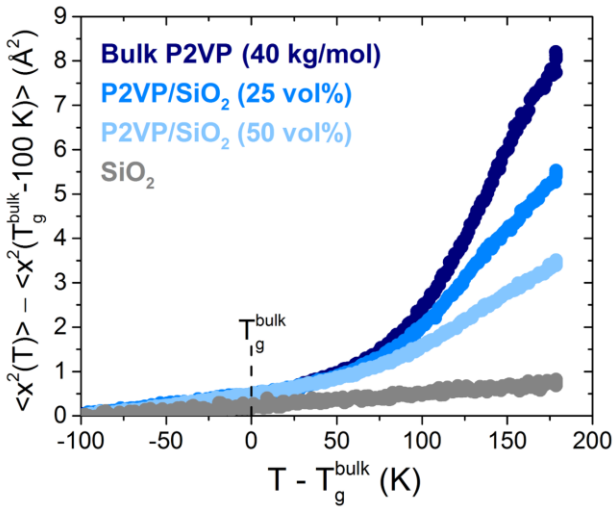

Figure 3: Average segmental mean-squared displacement (MSD) obtained from FWS of bulk 40 kg/mol P2VP and P2VP/SiO_2 PNCs with concentrations of 25 and 50 vol%. MSD is defined relative to T_g-100 K and temperature is defined relative to bulk calorimetric T_g. The MSD of nuclei in dried SiO_2 are shown for comparison and display expected linear Debye-like thermal motion.

P2VP segments in bulk and PNCs show similar low mobility for $T < T_g$, consistent with thermal harmonic vibrations in the glassy state.[43] For $T > T_g$, polymer segments exhibit a dramatic increase in $\langle x^2 \rangle$ as they become more mobile and are able to relax in the melt state. The bulk polymer and both PNCs show the change in slope occurring at similar $T\text{-}T_g^{bulk}$, as expected from the small increase in calorimetric T_g with the addition of NPs. However, at $T>T_g$, polymer segments in P2VP/SiO_2 PNCs show significantly reduced mobility with increasing NP concentration. Also shown in Figure 3 is a sample of SiO_2 NPs for comparison. Because the incoherent scattering cross-sections of hydrogen (σ_{inc}^{H} ~ 80 barns) is much larger than Si (σ_{inc}^{Si} ~ 0 barns and σ_{coh}^{Si} ~ 2.1 barns) and O (σ_{inc}^{O} ~ 0 barns and σ_{coh}^{O} ~ 4.2 barns), we expect the SiO_2 signal to be

dominated by hydrogens in surface hydroxyl groups.[38] The MSD of nuclei in the dried SiO_2 NPs show no change of slope and minimal mobility over all temperatures, as expected from thermal vibrations.[44,45]

Figure 3 shows the overall mobility of hydrogens in the sample but it is difficult to separate various types of polymer motion by monitoring only the elastic scattering intensity. For example, any protons mobile on the experimental length and time scale will contribute to $\langle x^2 \rangle$, regardless of their motion being diffusion, reorientations, rotations, or other motions. To better understand and characterize the segmental mobility and dynamic processes, isothermal QENS measurements of $S_S(q,\omega)$ were made. According to Figure 3, measurement temperatures of at least $\sim T_g$+100 K will place segmental dynamics in the experimental length and time scale. Figure 4a shows a representative QENS spectrum of bulk 40 kg/mol P2VP at 550 K and q=1.21 $Å^{-1}$ and is compared to P2VP with NP concentration of 25 and 50 vol% in Figure S4.

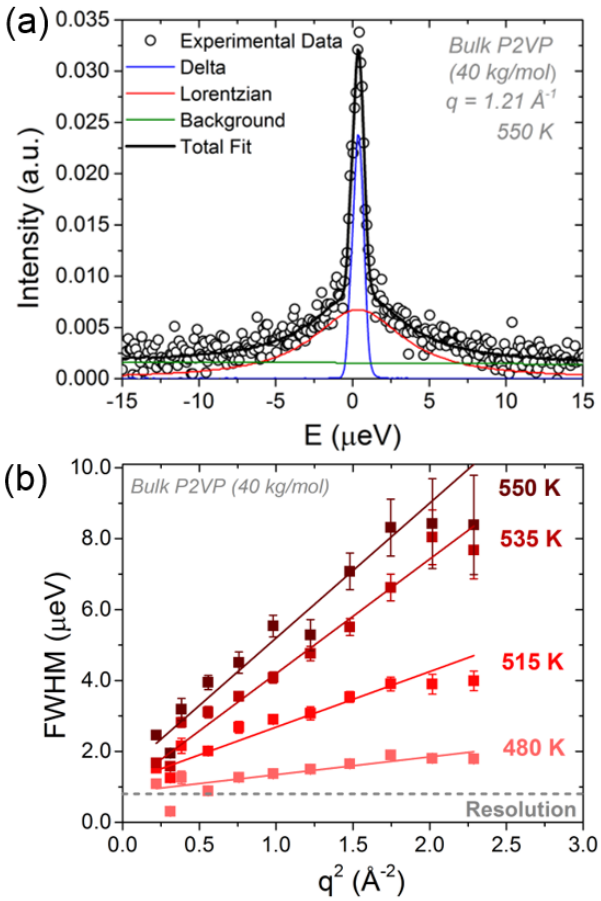

Figure 4: (a) Representative fit of experimental QENS spectra for bulk 40 kg/mol P2VP at 550 K (T_g+180 K) and q=1.21 Å^{-1}. (b) Quasi-elastic broadening (full width at half max of Lorentzian contribution) plotted as a function of q^2 for bulk P2VP at different temperatures. Measured broadening surpasses experimental resolution and clearly displays linear dependence, indicative of translational diffusive motions.

As shown in Figure 4a, a delta function is used to describe the elastic contribution, or signal from protons not moving within the experimental time window and length scale. A single Lorentzian is used to describe the quasi-elastic broadening (dynamics) and a linear function is included to represent background signal and dynamics much faster than the time window. The experimental data is fit by the linear combination of each contribution after convolution with a Gaussian representing experimental resolution. With this relatively simple single Lorentzian model, the data show no significant or systematic residuals (Figure S4) and therefore more complex models, such as the addition of another Lorentzian, are unwarranted.

Figure 4b shows the full width at half max (FWHM) of the Lorentzian component for bulk 40 kg/mol P2VP plotted as a function of q^2 for several temperatures. The quasi-elastic broadening is found to

increase linearly with q^2, indicative of translational diffusive motions where the slope is related to the diffusion coefficient ($FWHM \sim Dq^2$).[46] One may expect signatures of Rouse dynamics at low q (where $FWHM \sim q^4$)[25,46], but this is not apparent in our data. With a Kuhn segment length of ~1-2 nm for P2VP, the length scales probed by QENS are likely smaller than those associated with Rouse dynamics.[47] The apparent non-zero y-intercept in Figure 4b is expected from the presence of q-independent reorientational motions (such as pyridine ring fluctuations or β-relaxations) as well as potential contributions from multiple scattering events, which are expected to be minimal for the present sample dimensions. More complex models, such as jump diffusion[46], are often applied to polymeric systems but do not appreciably improve the fits as compared to the translational diffusion model for both bulk P2VP and PNCs. Importantly, the observed quasi-elastic broadening is substantially larger than the energy resolution, especially for $T \geq 515$ K. As expected, at higher temperatures, the observed FWHM increases as segmental mobility increases.

Using 535 K as an example, Figure 5a shows the quasi-elastic broadening is reduced with increasing SiO_2 NP concentration. The q-dependence of the FWHM for all systems and all measurement temperatures are included in Figure 4b and S5. Using the translational diffusion model, the segmental diffusion coefficients (D_α) were extracted from the slope of Figure 5a and are plotted as a function of inverse temperature in Figure 5b. These extracted diffusion coefficients can be directly compared to TMDSC and BDS through $\tau \sim (D_\alpha q^2)^{-1}$ where a q of 0.63 $Å^{-1}$ was chosen. As shown in Figure 1, the measured QENS relaxations times for bulk 40 kg/mol P2VP at $T > 515$ K are consistent with BDS and TMDSC measurements, suggesting that the observed dynamics are related to the primary structural relaxation process. A detailed discussion of analysis for BDS measurements and a comparison to literature is provided in Section 7 of Supporting Information.

At the high measurement temperatures ($T > T_g+100$ K) and over the narrow temperature range studied by QENS, D_α shows Arrhenius behavior for bulk and PNC materials (Figure 5b). Although $D_{\alpha,PNC} < D_{\alpha,Bulk}$, all materials exhibit similar activation energies. The effect of NP concentration is further highlighted by normalizing D_α relative to bulk measurements at the same temperature (Figure 5c) showing

a monotonic decrease in the average polymer segmental diffusion coefficient with increasing NP concentration. Specifically, D_α drops by ~40% with 25 vol% NP and ~80% with 50 vol% NP concentration when P2VP is lightly entangled. Furthermore, over the narrow temperature range measured, the reduction in diffusion coefficient is independent of temperature within experimental error. This slowing of segmental dynamics with increased NP concentration is consistent with the increase in T_g (Figure 2) and decrease in MSD for all $T>T_g$ (Figure 3), despite the isolation of diffusive motions of protons.

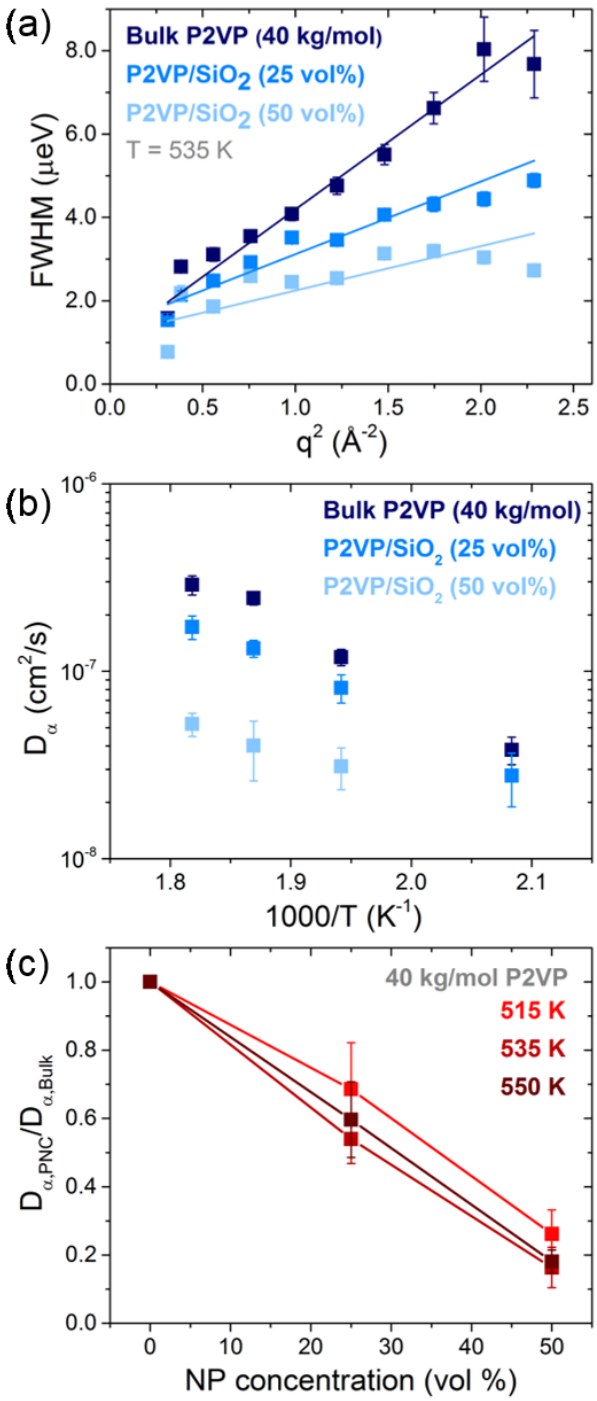

Figure 5: (a) FWHM of P2VP and P2VP/SiO_2 PNCs as a function of q^2 for measurements at 535 K. (b) Translational segmental diffusion coefficient as a function of temperature for all 40 kg/mol bulk and PNC measurements. (c) Reduced segmental diffusion coefficient (relative to bulk) as a function of NP concentration.

Assuming monodisperse NPs randomly dispersed in the polymer matrix, the average interparticle distance (ID) is given as $ID=d_{NP}\left[\left(2/\left(\pi\phi_{NP}\right)\right)^{1/3}-1\right]$ where d_{NP} and ϕ_{NP} are the NP diameter and volume fraction, respectively.[48] Thus, at ϕ_{NP} = 25 and 50 vol%, ID is ~9.5 nm and ~2.2 nm, respectively. From dynamic and static measurements from various techniques, the length scale of the perturbed interfacial layer (from the perspective of segmental dynamics) is often reported as ~2-5 nm from the NP surface.[15] As such, to a first approximation, the 50 vol% PNC can be considered an "all-interfacial" PNC wherein nearly all of the polymer segments are within the interfacial layer. Therefore, Figure 5c suggests that the interfacial layer in this strongly attractive PNC system is dynamically active at these high temperatures and the measured segmental diffusion coefficient from QENS is slowed by nearly one order of magnitude.

Effect of chain length on interfacial dynamics: To study the effect of molecular weight on interfacial dynamics, we studied PNCs with 25 vol% SiO_2 dispersed in P2VP with molecular weights ranging from unentangled to well-entangled (10, 40, and 190 kg/mol), Table 1. The results from FWSs for each polymer and PNC are shown in Figure 6. To account for the molecular weight dependence of T_g^{bulk} (Figure 2), $\langle x^2 \rangle$ is normalized to $T=T_g^{bulk} - 100$ K and temperature is presented relative to T_g^{bulk}. Data from all three MWs essentially collapse onto a master curve for bulk polymer and 25 vol% PNCs, showing that segmental mobility is largely independent of molecular weight (even in the case of PNCs).

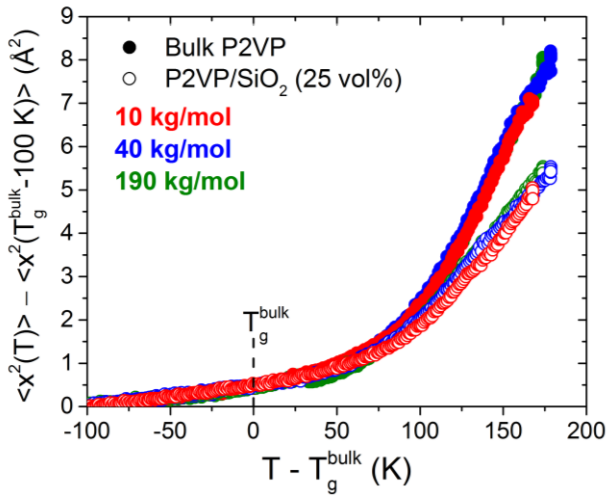

Figure 6: Average mean-squared displacement of segments for different polymer molecular weights as a function of temperature. MSD is presented relative to T_g^{bulk} – 100 K as a function of temperature relative to T_g^{bulk}.

Isothermal QENS measurements were performed at 525, 535, and 535 K for PNCs and bulk polymers with MWs of 10, 40, and 190 kg/mol, respectively. At these temperatures, which are all ~T_g^{bulk}+160 K, segments in bulk exhibit a similar average MSD (~7 Å^2 relative to $\langle x^2 \rangle$ at T=50 K), as shown in Figure S3. Given the weak temperature dependence of $D_{\alpha,PNC}$ / $D_{\alpha,Bulk}$ (Figure 5c), we will compare these QENS measurements as isothermal.

All bulk and PNC materials exhibit classic characteristics of translational segmental diffusion (FWHM ~ $D_\alpha q^2$), as shown in Figure 5a and Figure S7. Figure 7a shows that D_α for bulk P2VP is approximately independent of MW, differing by less than 30% from each other. Small variations in bulk D_α are attributed to slight differences in measurement temperature relative to T_g (Table 1, Figure 2) and fragility. The measured D_α values for 25 vol% PNCs are also shown in Figure 7a and the segmental diffusion coefficients are significantly suppressed upon the addition of attractive NPs.

To quantitatively compare the impact of molecular weight on segmental diffusion in PNCs, $D_{\alpha,PNC}$ is normalized by $D_{\alpha,Bulk}$ in Figure 7b. The error bars in Figure 7b represent the propagated error in fitting the q^2 dependence of the quasi-elastic broadening and do not include the errors associated with small differences in NP concentration, measurement temperatures, etc. For all molecular weights of P2VP, the addition of 25 vol% SiO_2 NPs causes a substantial reduction in the average segmental diffusion coefficient.

For PNCs with 10 kg/mol and 190 kg/mol P2VP, $D_{\alpha,PNC}/D_{\alpha,bulk}$ is 42±5% (T=525 K) and 61±8% (T=535 K), respectively. These conclusions are similar to those from the FWS presented in Figure 6, that the addition of NPs significantly reduces the segmental dynamics in PNCs but the effect is weakly dependent on molecular weight. In contrast, a much stronger molecular weight dependence was observed in the difference between T_g in PNCs and bulk (ΔT_g): 4.2 K for 10 kg/mol and 0.5 for 190 kg/mol (Figure 2). In addition, at the highest molecular weight of 190 kg/mol, although T_g approaches the bulk value, the dynamics measured by QENS at high temperature are still measurably reduced.

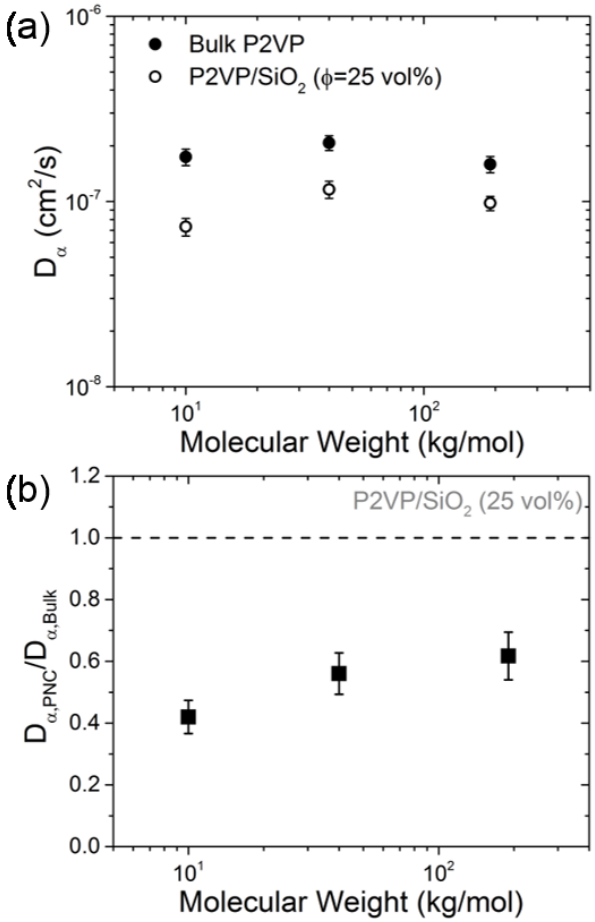

Figure 7: (a) Measured diffusion coefficient as a function of molecular weight for bulk and 25 vol% PNCs. (b) Reduced diffusion coefficient as a function of polymer molecular weight.

Discussion:

These QENS measurements at high temperatures correspond to time and space correlations at fast time scales (~1 ns) and short length scales (< ~2 nm). In this regime, we observed that the time scale of polymer relaxation increases with the length scale squared, consistent with translational diffusive motion. We expect that the observed diffusion process is dominated by the primary structural relaxation (α-process), rather than a secondary relaxation (β-process).[28,29,49,50] Unlike our observations of slower segmental dynamics in PNCs, recent neutron and light scattering measurements showed β-relaxations faster than bulk in P2VP/SiO_2 PNCs at 300 K.[28] Our α-process assignment is further supported by the agreement between TMDSC, BDS, and QENS measurements of bulk P2VP in Figure 1. Note that the α- and β-processes are expected to converge at high temperatures, but BDS, NMR, or QENS measurements at lower temperatures might be able to separate their contributions.

The bulk polymer and PNCs in our measurements exhibit similar q^2-dependence of quasielastic broadening, differing only in the value of the observed segmental diffusion coefficient (Figure 5c). Surprisingly, this suggests that the measured dynamics are significantly perturbed temporally and relatively unperturbed spatially in our q-range corresponding to ~0.5 – 2 nm. It is reasonable to expect segments beyond 2 nm from the NP surface to relax spatially bulk-like (from the perspective of QENS) because their local environment is similar to bulk polymer. Since most segments, especially in PNCs with 25 vol% NPs (ID~9.5 nm), are far enough from the NP surface, our measurements show no significant changes in the q^2-dependence of the dynamics. To further confirm this hypothesis, measurements over a larger q-range are necessary. Nevertheless, since we observe temporal perturbations without spatial perturbations, our results imply that the impact of a NP surface is farther ranging temporally than spatially.

The reduction in normalized D_α with increased concentration of attractive NPs measured by QENS at high temperatures (Figure 5c) captures the slow segmental motion observed in BDS[29] and TMDSC (Figure 2). In BDS, the mean molecular relaxation time in similar PNCs is nominally unchanged[51] and requires detailed analysis to reveal a second relaxation that is nearly two orders of magnitude slower.[52] In

contrast, our QENS analysis provides an average diffusion coefficient that is significantly reduced suggesting that this method is insensitive to the faster diffusion corresponding to bulk-like P2VP. Others have reported similar findings when comparing inelastic neutron scattering and other techniques, including NMR[26] and ellipsometry[45]. This has been explained by differences in dynamic sampling, wherein inelastic neutron scattering is biased to the slower processes.[45] This is consistent with our data. We extract an average diffusion coefficient in PNC systems that is slower than that of bulk, even when the interparticle distance is nearly 10x larger than the measurement length scale. The discrepancy between neutron scattering and other techniques has also been described in terms of technique sensitivity and dynamic range, where the spectral shape is analyzed over only one order of magnitude in QENS (Figure 1). This is also consistent with our PNC data being described by a single Lorentzian, despite the known heterogenous dynamic environment PNCs. Our direct comparison of TMDSC and QENS, along with similar measurements from BDS[29], demonstrate that considering differences in experimental probes and sensitivities is critical in future comparisons, especially in heterogeneous materials such as PNCs.

In QENS, when a segment relaxes slower than the experimental time scale (~2 ns), it appears immobile and therefore contributes to the elastic peak and is excluded from the QENS broadening analysis. This effect can be directly quantified by the elastic incoherent structure factor (EISF), which represents the fraction of immobile nuclei and is calculated by the area of the elastic contribution relative to the sum of the elastic and quasielastic contributions. The EISF for each sample measured at ~T_g+160 K is shown as a function of q in Figure 8a. For each bulk sample, nearly 80% of segments are mobile at q ~ 1 $Å^{-1}$ but upon the addition of NPs, a smaller fraction of nuclei are mobile on this nanosecond time scale. Thorough analysis and fitting of the q-dependence of the EISF is beyond the scope of this study, but it is worth noting that our data follows a similar trend to comparable systems in literature.[20,46]

The addition of hydroxyl-terminated SiO_2 NPs introduces additional scattering intensity that will contribute to the elastic fraction and therefore affect the EISF. To account for this contribution, we assume an upper estimate for the hydroxyl surface density of ~4.9 nm^{-2} and amorphous SiO_2 and P2VP densities of 2.3 and 1.2 g/cm^3, respectively, and calculate the predicted incoherent and coherent scattering intensities of

each sample using Equation 2.[38,53] For NP loadings of 25 and 50 vol%, the polymer scattering accounts for 83% and 63% of the total scattering contributions. It is important to note that the incoherent and coherent scattering from SiO_2 does not affect the measured quasielastic broadening or D_α because the nuclei are immobile on the experimental length and time scales (Figure 3) and therefore contribute solely to the elastic scattering. This increase in elastic scattering was accounted for in the EISF, but in all samples, the reduction in mobile nuclei was found to be more than expected from just the addition of SiO_2 NPs. This difference can be attributed to nuclei of the polymer that are slowed beyond the temporal window of the experiment and therefore appear immobile, most likely belonging to segments closest to the attractive NP interface.

Using a simple three-phase model including SiO_2, immobile polymer, and mobile polymer, the "interfacial width" can be extracted by correlating the measured fraction of immobile polymer to the increased NP-polymer interfacial volume resulting from increased NP concentration. The calculated interfacial width is shown in Figure 8b, where the error bars represent the standard deviation of calculations for $0.55 < q < 1.6$ Å^{-1}. The interfacial with is ~1 nm and is independent of NP loading (see 40 kg/mol) and molecular weight. This interfacial width does not delineate the slow segments from the bulk-like segments because the remaining segments are still slower than bulk (Figure 5c). Instead, this interfacial width represents the estimated average distance from the NP surface after which segments relax within the window of QENS. Without accounting for scattering from SiO_2 NPs, the interfacial width falsely appears to be ~2.5 nm but the MW dependence remains unchanged.

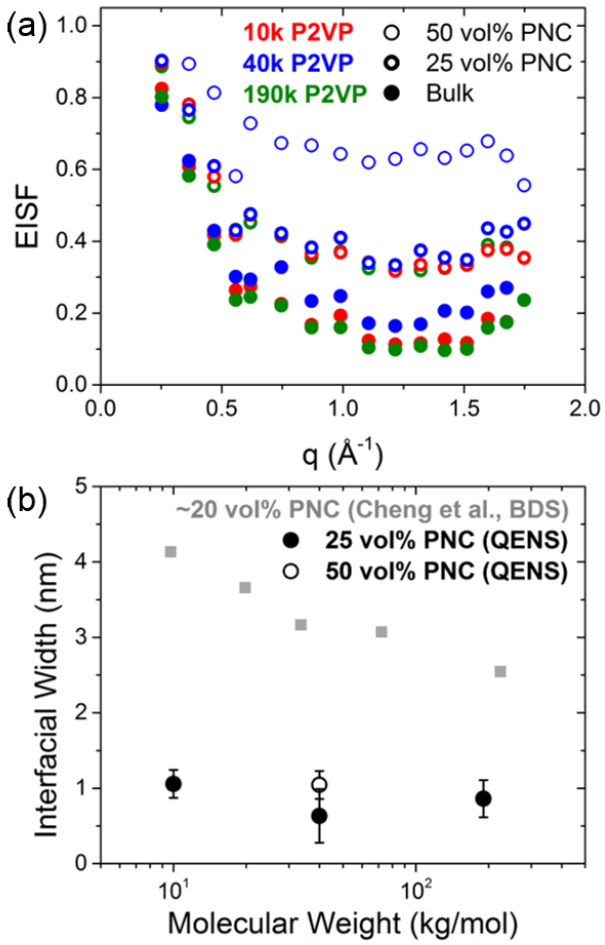

Figure 8: (a) Elastic incoherent structure factor versus q for all bulk and PNC samples measured at ~T_g+160 K. (b) Extracted interfacial width of segments immobile on the experimental length and time scale. Gray squares are BDS measurements adopted from Cheng et al.[33]

The extracted interfacial widths via BDS[33] and QENS (Figure 8b) show surprisingly distinct molecular weight dependences. Whereas the interfacial thickness in BDS decreases from ~4 nm at low MW to ~2.5 nm at high MW (consistent with arguments of MW-dependent interfacial packing[31,33]), the interfacial thickness in QENS is consistently ~1 nm over the same molecular weight range. Although these are structural insights inferred from dynamic measurements, the same behavior is observed in direct measurements of segmental dynamics. In TMDSC (Figure 2) and BDS[33] measurements, the increase in glass transition temperature and decrease in segmental dynamics (respectively) are highly dependent on matrix MW, whereas we observed that $D_{\alpha,PNC}/D_{\alpha,Bulk}$ in QENS is nearly independent of molecular weight.

Although QENS, TMDSC, and BDS probe the same dynamic process (Figure 1), a notable difference between these experimental methods is the measurement temperature, which has two important implications. First, it remains unclear how the structure, dynamics, and interactions of the interfacially bound polymer segments depend on temperature. Thus, TMDSC ($T \sim T_g$), BDS ($T < T_g + 60$ K) and QENS ($T \sim T_g + 160$ K) may probe fundamentally different perturbations to the segmental dynamic process. Limited experimental data suggests a reduced interfacial width at elevated temperatures, which is in line with the observations in Figure 8b.[15] Second, the loops and trains of the adsorbed polymers may depend on processing conditions, even after long annealing.[15] In fact, processing details including concentrations of polymer and NP solutions, solvent quality, and annealing conditions, may impact the adsorbed polymer conformations and subsequently the interfacial dynamics. As such, it is important for the field to consider and clearly report these details. At elevated temperatures, not only is the entropy of interfacial chains promoted and local free volume increased, but the relative strength of the hydrogen bond is decreased. Samples measured for several hours at the high temperatures as required for QENS may provide enough time and thermal energy for segments to sample their local environment and energetic landscape and reach a more equilibrium conformation. Future studies of annealing time and temperature are needed to fully understand the influence of processing on interfacial dynamics.

Not only can QENS provide complimentary dynamic measurements to other techniques but it offers several unique capabilities, making it a useful complement to the field of segmental dynamics in PNCs. In this work, the use of spatial correlations in bulk and PNCs showed that although the observed segmental dynamics are temporally slowed, they are relatively unperturbed spatially. The fast time scales probed by QENS captures dynamics at elevated temperatures to elucidate the role of temperature on interfacial segmental dynamics. In addition, the ability to quantify the fraction of mobile and immobile species allowed the extraction of structural parameters from dynamic measurements. Finally, unique capability of neutron scattering that has yet to be fully exploited is selective H/D labeling to isolate and investigate different polymer dynamics and processes within the chain (through intrachain deuteration) or spatially in the PNC (through interchain deuteration).

Conclusion:

Quasi-elastic neutron scattering was used to study segmental dynamics in highly attractive polymer nanocomposites (PNCs) at high temperatures (~T_g+150 K). We isolate the role of nanoparticle (NP) concentration, temperature, and matrix molecular weight on segmental dynamics in model PNCs made of P2VP and 26 nm colloidal SiO_2. We monitor the elastic scattering as a function of temperature to reveal proton mobility over a wide temperature range and measure the dynamic structure factor under isothermal conditions to probe dynamics on length and time scales of ~ 1 nm and ~ 1 ns, respectively. We show segmental mobility is strongly reduced for all $T>T_g$ upon the addition of NPs. At the QENS length and time scales, we observe classic translational diffusion of segments in bulk and in PNCs, even when the average interparticle separation distance is ~2 nm (50 vol% SiO_2). Simultaneously, the average segmental diffusion coefficient is reduced by ~80% (relative to bulk) at NP concentrations of 50 vol%, showing strong temporal suppression without spatial perturbations. Similar observations are made for PNCs with unentangled and well-entangled matrix polymers. The decrease in segmental mobility for all $T>T_g$ and a reduced diffusion coefficient are highly dependent on NP concentration, but nearly independent of matrix molecular weight.

Several dynamic probes have been used to study segmental dynamics in highly attractive PNC systems. By comparing our QENS results to solely dynamic measurements on slower time-scales (and therefore lower temperatures), we highlight categorically different observations on similar PNC systems. Namely, calorimetric measurements (measured at $T\sim T_g$) show a much stronger molecular weight dependence than QENS (measured at $T>>T_g$). These discrepancies provide insights into the effect of temperature on the observed segmental dynamics in attractive PNCs. Furthermore, the unique ability of space and time correlations and selective labeling in neutron scattering presents a valuable future direction to mechanistically understand segmental diffusion in various PNC systems.

Associated Content:

Supporting Information:

Representative TEM images of 40 kg/mol PNCs, thermogravimetric curves for bulk polymer, raw FWS for each sample and discussion of FWS analysis, representative fits to QENS spectra of PNC, q^2-dependence of quasi-elastic broadening for 40 kg/mol PNCs at all temperatures, discussion of BDS analysis, q^2-dependence of quasi-elastic broadening for PNCs of all molecular weights, and discussion of thermal degradation of materials during QENS measurements.

Author Information:

Corresponding author:

*Email: winey@seas.upenn.edu (K.I.W.).

ORCID:

Eric J. Bailey: 0000-0001-7194-9035

Karen I. Winey: 0000-0001-5856-3410

Notes:

The authors declare no competing financial interest.

Acknowledgements:

EJB and KIW acknowledge support from NSF-CBET #1706014 and DOE-BES via DE-SC0016421. EJB acknowledges primary support from the National Science Foundation Graduate Research Fellowship Program under Grant No. DGE-1321851. Any opinions, findings, and conclusions or recommendations expressed in this material are those of the authors and do not necessarily reflect the views of the National Science Foundation. Access to high-flux backscattering spectrometer (HFBS) was provided by the Center for High Resolution Neutron Scattering, a partnership between the National Institute of Standards and Technology and the National Science Foundation under Agreement No. DMR-1508249. Certain commercial equipment, instruments, or materials are identified in this paper in order to specify the

experimental procedure adequately. Such identification is not intended to imply recommendation or endorsement by the National Institute of Standards and Technology, nor is it intended to imply that the materials or equipment identified are necessarily the best available for the purpose. Parts of this work were carried out at the Soft Matter Characterization Facility of the University of Chicago. The authors would like to thank Vera Bocharova for NP synthesis and graciously providing NP solutions. The authors would also like to thank Leshang Wang and Peter Gordon for GPC measurements of 190 kg/mol P2VP, Nadia M. Krook for assistance with TEM, and Steve Szewczyk for assistance with various measurements.

References:

(1) Winey, K. I.; Vaia, R. A. Polymer Nanocomposites. *MRS Bull.* **2007**, *32*, 314–322.
(2) Kumar, S. K.; Benicewicz, B. C.; Vaia, R. A.; Winey, K. I. 50th Anniversary Perspective: Are Polymer Nanocomposites Practical for Applications? *Macromolecules* **2017**, *50*, 714–731.
(3) Gam, S.; Meth, J. S.; Zane, S. G.; Chi, C.; Wood, B. a.; Seitz, M. E.; Winey, K. I.; Clarke, N.; Composto, R. J. Macromolecular Diffusion in a Crowded Polymer Nanocomposite. *Macromolecules* **2011**, *44* (9), 3494–3501.
(4) Lin, C.; Gam, S.; Meth, S.; Clarke, N.; Winey, K. I.; Composto, R. J. Do Attractive Polymer − Nanoparticle Interactions Retard Polymer Diffusion in Nanocomposites? *Macromolecules* **2013**, *46*, 4502–4509.
(5) Choi, J.; Hore, M. J. a; Meth, J. S.; Clarke, N.; Winey, K. I.; Composto, R. J. Universal Scaling of Polymer Diffusion in Nanocomposites. *ACS Macro Lett.* **2013**, *2* (6), 485–490.
(6) Choi, J.; Clarke, N.; Winey, K. I.; Composto, R. J. Fast Polymer Diffusion through Nanocomposites with Anisotropic Particles. *ACS Macro Lett.* **2014**, *3* (9), 886–891.
(7) Mu, M.; Composto, R. J.; Clarke, N.; Winey, K. I. Minimum in Diffusion Coefficient with Increasing MWCNT Concentration Requires Tracer Molecules to Be Larger than Nanotubes. *Macromolecules* **2009**, *42* (21), 8365–8369.
(8) Mu, M.; Clarke, N.; Composto, R. J.; Winey, K. I. Polymer Diffusion Exhibits a Minimum with Increasing Single-Walled Carbon Nanotube Concentration. *Macromolecules* **2009**, *42* (18), 7091–7097.
(9) Mu, M.; Seitz, M. E.; Clarke, N.; Composto, R. J.; Winey, K. I. Polymer Tracer Diffusion Exhibits a Minimum in Nanocomposites Containing Spherical Nanoparticles. *Macromolecules* **2011**, *44* (2), 191–193.
(10) Lin, C. C.; Parrish, E.; Composto, R. J. Macromolecule and Particle Dynamics in Confined Media. *Macromolecules* **2016**, *49* (16), 5755–5772.
(11) Ozisik, R.; Zheng, J.; Dionne, P. J.; Picu, C. R.; Von Meerwall, E. D. NMR Relaxation and Pulsed-Gradient Diffusion Study of Polyethylene Nanocomposites. *J. Chem. Phys.* **2005**, *123* (13).
(12) Robertson, C. G.; Roland, C. M. Glass Transition and Interfacial Segmental Dynamics in Polymer-Particle Composites. *Rubber Chem. Technol.* **2008**, *81* (3), 506–522.
(13) Schneider, G. J. Dynamics of Nanocomposites. *Curr. Opin. Chem. Eng.* **2017**, *16*, 65–77.
(14) Priestley, R. D.; Cangialosi, D.; Napolitano, S. On the Equivalence between the Thermodynamic and Dynamic Measurements of the Glass Transition in Confined Polymers. *J. Non. Cryst. Solids* **2015**, *407*, 288–295.
(15) Cheng, S.; Carroll, B.; Bocharova, V.; Carrillo, J.-M.; Sumpter, B. G.; Sokolov, A. P. Focus: Structure and Dynamics of the Interfacial Layer in Polymer Nanocomposites with Attractive Interactions. *J. Chem. Phys.* **2017**, *146* (20), 203201.
(16) Genix, A.-C.; Oberdisse, J. Structure and Dynamics of Polymer Nanocomposites Studied by X-Ray and Neutron Scattering Techniques. *Curr. Opin. Colloid Interface Sci.* **2015**, *20* (4), 293–303.
(17) Kremer, F.; Schonhals, A. *Broadband Dielectric Spectroscopy*, 1st ed.; Springer: New York, 2003.
(18) Triolo, A.; Lo Celso, F.; Negroni, F.; Arrighi, V.; Qian, H.; Lechner, R. E.; Desmedt, A.; Pieper, J.; Frick, B.; Triolo, R. QENS Investigation of Filled Rubbers. *Appl. Phys. A Mater. Sci. Process.* **2002**, *74* (SUPPL.I), 490–492.
(19) Roh, J. H.; Tyagi, M.; Hogan, T. E.; Roland, C. M. Space-Dependent Dynamics in 1,4-Polybutadiene Nanocomposite. *Macromolecules* **2013**, *46* (16), 6667–6669.
(20) Chrissopoulou, K.; Anastasiadis, S. H.; Giannelis, E. P.; Frick, B. Quasielastic Neutron Scattering of Poly(Methyl Phenyl Siloxane) in the Bulk and under Severe Confinement. *J. Chem. Phys.* **2007**, *127* (14).
(21) Anastasiadis, S. H.; Chrissopoulou, K.; Frick, B. Structure and Dynamics in Polymer/Layered Silicate Nanocomposites. *Mater. Sci. Eng. B Solid-State Mater. Adv. Technol.* **2008**, *152* (1–3), 33–39.

(22) Kropka, J. M.; Garcia Sakai, V.; Green, P. F. Local Polymer Dynamics in Polymer− C60 Mixtures. *Nano Lett.* **2008**, *8* (4), 1061–1065.
(23) Arrighi, V.; Higgins, J. S.; Burgess, A. N.; Floudas, G. Local Dynamics of Poly(Dimethyl Siloxane) in the Presence of Reinforcing Filler Particles. *Polymer.* **1998**, *39* (25), 6369–6376.
(24) Akcora, P.; Kumar, S. K.; García Sakai, V.; Li, Y.; Benicewicz, B. C.; Schadler, L. S. Segmental Dynamics in PMMA-Grafted Nanoparticle Composites. *Macromolecules* **2010**, *43* (19), 8275–8281.
(25) Senses, E.; Faraone, A.; Akcora, P. Microscopic Chain Motion in Polymer Nanocomposites with Dynamically Asymmetric Interphases. *Sci. Rep.* **2016**, *6*, 29326;
(26) Glomann, T.; Schneider, G. J.; Allgaier, J.; Radulescu, A.; Lohstroh, W.; Farago, B.; Richter, D. Microscopic Dynamics of Polyethylene Glycol Chains Interacting with Silica Nanoparticles. *Phys. Rev. Lett.* **2013**, *110* (17), 1–5.
(27) Senses, E.; Tyagi, M.; Natarajan, B.; Narayanan, S.; Faraone, A. Chain Dynamics and Nanoparticle Motion in Attractive Polymer Nanocomposites Subjected to Large Deformations. *Soft Matter* **2017**.
(28) Holt, A. P.; Bocharova, V.; Cheng, S.; Kisliuk, A. M.; Ehlers, G.; Mamontov, E.; Novikov, V. N.; Sokolov, A. P. Interplay between Local Dynamics and Mechanical Reinforcement in Glassy Polymer Nanocomposites. *Phys. Rev. Mater.* **2017**, *1* (6), 062601.
(29) Holt, A. P.; Griffin, P. J.; Bocharova, V.; Agapov, A. L.; Imel, A. E.; Dadmun, M. D.; Sangoro, J. R.; Sokolov, A. P. Dynamics at the Polymer/Nanoparticle Interface in Poly(2-Vinylpyridine)/ Silica Nanocomposites. *Macromolecules* **2014**, *47* (5), 1837–1843.
(30) Griffin, P. J.; Bocharova, V.; Middleton, L. R.; Composto, R. J.; Clarke, N.; Schweizer, K. S.; Winey, K. I. Influence of the Bound Polymer Layer on Nanoparticle Diffusion in Polymer Melts. *ACS Macro Lett.* **2016**, *5* (10), 1141–1145.
(31) Voylov, D. N.; Holt, A. P.; Doughty, B.; Bocharova, V.; Meyer, H. M.; Cheng, S.; Martin, H.; Dadmun, M.; Kisliuk, A.; Sokolov, A. P. Unraveling the Molecular Weight Dependence of Interfacial Interactions in Poly(2-Vinylpyridine)/Silica Nanocomposites. *ACS Macro Lett.* **2017**, *6* (2), 68–72.
(32) Gong, S.; Chen, Q.; Moll, J. F.; Kumar, S. K.; Colby, R. H. Segmental Dynamics of Polymer Melts with Spherical Nanoparticles. *ACS Macro Lett.* **2014**, *3* (8), 773–777.
(33) Cheng, S.; Holt, A. P.; Wang, H.; Fan, F.; Bocharova, V.; Martin, H.; Etampawala, T.; White, B. T.; Saito, T.; Kang, N. G.; et al. Unexpected Molecular Weight Effect in Polymer Nanocomposites. *Phys. Rev. Lett.* **2016**, *116* (3), 1–5.
(34) Holt, A. P.; Bocharova, V.; Cheng, S.; Kisliuk, A. M.; White, B. T.; Saito, T.; Uhrig, D.; Mahalik, J. P.; Kumar, R.; Imel, A. E.; et al. Controlling Interfacial Dynamics: Covalent Bonding versus Physical Adsorption in Polymer Nanocomposites. *ACS Nano* **2016**, *10* (7), 6843–6852.
(35) Kamiya, H.; Suzuki, H.; Kato, D.; Jimbo, G. Densification of Alkoxide-Derived Fine Silica Powder Compact by Ultra-High-Pressure Cold Isostatic Pressing. *J. Am. Ceram. Soc.* **1993**, *76* (1), 54–64.
(36) Iijima, M.; Kamiya, H. Layer-by-Layer Surface Modification of Functional Nanoparticles for Dispersion in Organic Solvents. *Langmuir* **2010**, *26* (23), 17943–17948.
(37) Jouault, N.; Moll, J. F.; Meng, D.; Windsor, K.; Ramcharan, S.; Kearney, C.; Kumar, S. K. Bound Polymer Layer in Nanocomposites. *ACS Macro Lett.* **2013**, *2* (5), 371–374.
(38) Sears, V. F. Neutron Scattering Lengths and Cross Sections. *Neutron News* **1992**, *3* (3), 26–37.
(39) Ryong-Joon, R. *Methods of X-Ray and Neutron Scattering in Polymer Science*; Oxford University Press: New York, 2000.
(40) Meyer, A.; Dimeo, R. M.; Gehring, P. M.; Neumann, D. A. The High-Flux Backscattering Spectrometer at the NIST Center for Neutron Research. *Rev. Sci. Instrum.* **2003**, *74* (5), 2759–2777.
(41) Azuah, R. T.; Kneller, L. R.; Qiu, Y.; Tregenna-Piggott, P. L. W.; Brown, C. M.; Copley, J. R. D.; Dimeo, R. M. DAVE: A Comprehensive Software Suite for the Reduction, Visualization, and

Analysis of Low Energy Neutron Spectroscopic Data. *J. Res. Natl. Inst. Stand. Technol.* **2009**, *114* (6), 341.
(42) Elmaci, A.; Hacaloglu, J. Thermal Degradation of Poly(Vinylpyridine)S. *Polym. Degrad. Stab.* **2009**, *94* (4), 738–743.
(43) Inoue, R.; Kanaya, T.; Nishida, K.; Tsukushi, I.; Telling, M. T. F.; Gabrys, B. J.; Tyagi, M.; Soles, C.; Wu, W. L. Glass Transition and Molecular Mobility in Polymer Thin Films. *Phys. Rev. E - Stat. Nonlinear, Soft Matter Phys.* **2009**, *80* (3), 1–4.
(44) Soles, C. L.; Douglas, J. F.; Wu, W. L.; Dimeo, R. M. Incoherent Neutron Scattering as a Probe of the Dynamics in Molecularly Thin Polymer Films. *Macromolecules* **2003**, *36* (2), 373–379.
(45) Ye, C.; Wiener, C. G.; Tyagi, M.; Uhrig, D.; Orski, S. V.; Soles, C. L.; Vogt, B. D.; Simmons, D. S. Understanding the Decreased Segmental Dynamics of Supported Thin Polymer Films Reported by Incoherent Neutron Scattering. *Macromolecules* **2015**, *48* (3), 801–808.
(46) Springer, T. *Quasielastic Neutron Scattering for the Investigation of Diffusive Motions in Solids and Liquids*; Spinger-Verlag: Berlin and Heidelberg, Germany, 1972.
(47) Cheng, S.; Carroll, B.; Lu, W.; Fan, F.; Carrillo, J. M. Y.; Martin, H.; Holt, A. P.; Kang, N. G.; Bocharova, V.; Mays, J. W.; et al. Interfacial Properties of Polymer Nanocomposites: Role of Chain Rigidity and Dynamic Heterogeneity Length Scale. *Macromolecules* **2017**, *50* (6), 2397–2406.
(48) Wu, S. Phase Structure and Adhesion in Polymer Blends: A Criterion for Rubber Toughening. *Polymer (Guildf).* **1985**, *26* (12), 1855–1863.
(49) Tonelli, A. E. Conformational Characteristics of Poly(2-Vinylpyridine). *Macromolecules* **1985**, *18* (12), 2579–2583.
(50) Papadopoulos, P.; Peristeraki, D.; Floudas, G.; Koutalas, G.; Hadjichristidis, N. Origin of Glass Transition of Poly(2-Vinylpyridine). A Temperature- and Pressure-Dependent Dielectric Spectroscopy Study. *Macromolecules* **2004**, *37* (21), 8116–8122.
(51) Holt, A. P.; Sangoro, J. R.; Wang, Y.; Agapov, A. L.; Sokolov, A. P. Chain and Segmental Dynamics of Poly (2-Vinylpyridine) Nanocomposites. *Macromolecules* **2013**, *46*, 4168.
(52) Carroll, B.; Cheng, S.; Sokolov, A. P. Analyzing the Interfacial Layer Properties in Polymer Nanocomposites by Broadband Dielectric Spectroscopy. *Macromolecules* **2017**, *50*, 6149–6163.
(53) Mueller, R.; Kammler, H. K.; Wegner, K.; Pratsinis, S. E. OH Surface Density of SiO2 and TiO2 by Thermogravimetric Analysis. *Langmuir* **2003**, *19* (1), 160–165.